

## Article

# Protective Effects of Naringenin against UVB Irradiation and Air Pollution-Induced Skin Aging and Pigmentation

Christina Österlund \*, Nina Hrapovic, Virginie Lafon-Kolb, Nahid Amini, Sandra Smiljanic  and Lene Visdal-Johnsen

Swedish Research and Innovation Lab, Oriflame Cosmetics AB, Fleminggatan 14, 112 26 Stockholm, Sweden; lene.visdal-johnsen@oriflame.com (L.V.-J.)

\* Correspondence: christina.osterlund@oriflame.com

**Abstract:** Both UVB irradiation and air pollution are major extrinsic factors causing premature aging of the skin, including sagging, wrinkles, and pigmentation spots. Naringenin, a naturally occurring flavanone, found in citrus fruits, and known for its good antioxidant and anti-inflammatory effects, was investigated for protective effects in human skin cells and reconstructed epidermis. The results showed that naringenin inhibits UVB-induced inflammation markers MMP1, MMP3, IL6, and GM-CSF, as well as pollution-induced MMP1 in human skin fibroblasts. Furthermore, naringenin inhibited the pollution-induced expression of the *CYP1A1* gene in human skin keratinocytes. In melanocytes and pigmented reconstructed epidermis, naringenin significantly downregulated several genes involved in melanogenesis, such as MITF, MLPH, and MYO5A. Additionally topical treatment with naringenin on pigmented reconstructed epidermis significantly decreased melanin production. In conclusion, this study demonstrates that naringenin could be a valuable ingredient in skincare products, protecting against the detrimental effects of both UVB and pollution on the skin.

**Keywords:** naringenin; natural ingredient; UV protection; pollution protection; pigmentation



**Citation:** Österlund, C.; Hrapovic, N.; Lafon-Kolb, V.; Amini, N.; Smiljanic, S.; Visdal-Johnsen, L. Protective Effects of Naringenin against UVB Irradiation and Air Pollution-Induced Skin Aging and Pigmentation. *Cosmetics* **2023**, *10*, 88. <https://doi.org/10.3390/cosmetics10030088>

Academic Editor: Agnieszka Feliczak Guzik

Received: 25 April 2023

Revised: 26 May 2023

Accepted: 30 May 2023

Published: 7 June 2023



**Copyright:** © 2023 by the authors. Licensee MDPI, Basel, Switzerland. This article is an open access article distributed under the terms and conditions of the Creative Commons Attribution (CC BY) license (<https://creativecommons.org/licenses/by/4.0/>).

## 1. Introduction

Skin, the largest organ of the human body, undergoes significant changes during the aging process, which is influenced by both genetic and environmental factors. Intrinsic aging, driven by genetic factors, results in the gradual breakdown of collagen and elastin fibers, leading to loss of skin elasticity and firmness. Extrinsic aging, on the other hand, is largely driven by environmental factors such as UV radiation and pollution [1–3].

The mechanisms underlying the effects of UV radiation and pollution on skin aging are complex and multifactorial. UV radiation generates reactive oxygen species (ROS) that contribute to the breakdown of collagen and elastin fibers in the skin, resulting in a loss of elasticity and firmness [4]. Exposure to pollution can also generate ROS and trigger inflammatory pathways, which can further exacerbate the effects of UV radiation and accelerate the aging process [5]. Notably, air pollution exposure has been shown to be correlated with the development of pigment spots [5,6].

Air pollution as well as UV radiation can activate the aryl hydrocarbon receptor (AhR) [7,8]. This, in turn, leads to the activation of downstream genes, such as *MMP1* and *CYP1A1*, resulting in increased production of ROS, inflammatory cytokines, and collagen breakdown [8–10].

Effective protection of the skin against the detrimental effects of both UV radiation and pollution is therefore essential to maintain healthy skin.

In recent years, there has been growing interest in the use of natural compounds in skincare products. One class of compounds that has gained considerable attention is flavonoids. Flavonoids are a diverse group of phytochemicals, widely distributed in fruits, vegetables, herbs, and medicinal plants, and are known for their various biological activities. In the

realm of skincare, flavonoids, such as quercetin, kaempferol, and rutin, are highly regarded for their potent antioxidant and anti-inflammatory properties [11–13]. Another promising area of application for flavonoids in skincare is their photoprotective potential. Flavonoids have demonstrated their capacity to absorb and scatter UV radiation, thus reducing its penetration into the skin and minimizing its harmful effects [14–16]. One particular flavonoid of interest is naringenin (5,7,4'-trihydroxyflavanone, depicted in Figure 1), which is abundantly found in citrus fruits. Several animal studies have indicated that naringenin holds immense potential in benefiting the skin through its photoprotective, anti-inflammatory, antioxidant, and skin-brightening effects [17–21]. These accumulated findings strongly suggest that naringenin may prove to be effective not only in shielding the skin against UV radiation-induced photoaging but also in protecting it from the harmful effects of pollution.

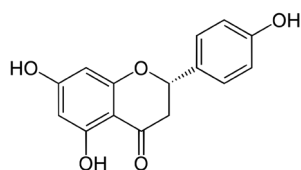


**Figure 1.** Chemical structure of naringenin.

The present study aims to (1) investigate the *in vitro* UV protective/anti-inflammatory effects of naringenin on human primary skin cells, (2) investigate naringenin's ability to protect against pollution-induced skin inflammation and oxidative stress in human skin cells, and (3) investigate naringenin's effect on melanogenesis genes and melanin production in human skin cells and reconstructed pigmented epidermis.

## 2. Materials and Methods

### 2.1. Viability

In parallel with all assays, viability testing was performed using CellTiterGlo (Promega, Madison, WI, USA) according to manufacturer's instructions.

### 2.2. Cell Culture

Primary human keratinocytes, fibroblasts, and melanocytes, all came from healthy female donors, 24–56 years of age (Cellsystems GmbH, Troisdorf, Germany). They were maintained in EpiLife supplemented with HKGS (Gibco, Grand Island, NY, USA), DMEM containing 10% fetal bovine serum (Gibco) or Media 254 supplemented with HMGS at 37 °C in a 5% CO<sub>2</sub> humidified incubator.

### 2.3. UVB Keratinocyte/Fibroblast Assay

The UVB keratinocyte/fibroblast assay is a paracrine assay where the media from UV stimulated primary keratinocytes is used to activate primary dermal fibroblasts (method adapted from Wang et al. [22]). Briefly, the keratinocytes were cultured until they reached approximately 80% confluence and then were irradiated with 50 mJ/cm<sup>2</sup> in the UVB range of 280–315 nm, using the UV-MAT Irradiation controller from Dr Gröbel GmbH, Ettlingen, Germany. The cells were then cultured at 37 °C in a 5% CO<sub>2</sub> humidified incubator, and the media was collected after 24 h. Fibroblasts were cultured to approximately 80% confluence and pretreated with naringenin, at 1.5 μM, 15 μM or 150 μM, (Sigma-Aldrich, St. Louis, MO, USA >95% purity) for 1 h before changing to the media from the UV-treated keratinocytes. After 24 h incubation the media was collected and analyzed using MMP1 ELISA (Sigma-Aldrich) or Luminex analysis (ProCartaPlex, Affymetrix, Santa Clara, CA, USA). Standard curve from the ELISA was plotted as log concentration vs. absorbance (-blank) and then analyzed with variable slope four parameter curve fit. Standard curve from the Luminex was plotted as log concentration vs. absorbance (-blank) and then analyzed with asymmetric five parameter curve fit according to manufacturer's instructions. Assay is considered valid when the biomarker in question is significantly higher after

stimulation than the untreated vehicle control. Cells are stimulated in parallel with IL1-beta (Sigma-Aldrich) and inhibited with IL-1 receptor antagonist (Sigma-Aldrich) as a functional assay control.

#### 2.4. Pollution-Induced Keratinocyte/Fibroblast Assay

The pollution-induced keratinocyte/fibroblast assay is a paracrine assay in which the media from keratinocytes stimulated with diesel particulate matter (DPM), is utilized to activate dermal fibroblasts.

Keratinocytes were cultured to approximately 80% confluence and then cultured in the presence of 10 µg/mL DPM (1650b, National Institute of Standards and Technology, Gaithersburg, MD, USA). The media was collected after 24 h. Fibroblasts were cultured to approximately 80% confluence and pretreated with 150 µM naringenin for 1 h before changing to the media from the DPM-treated keratinocytes in combination with 150 µM naringenin (Sigma-Aldrich). After 24 h incubation, the fibroblast media was collected and analyzed by MMP1 ELISA (Sigma-Aldrich) according to manufacturer's instructions. Standard curve from the ELISA was plotted as log concentration vs. absorbance (-blank) and then analyzed with variable slope four parameter curve fit. Assay is considered valid when the biomarker in question is significantly higher after stimulation than the untreated vehicle control. Cells are in parallel stimulated with IL1-beta, 100 ng/mL (Sigma-Aldrich), and inhibited with IL-1 receptor antagonist, 200 ng/mL (Sigma-Aldrich), as a functional assay control.

#### 2.5. Pollution-Induced CYP1A1 Assay

The pollution induced CYP1A1 assay is a qPCR assay analyzing *CYP1A1* gene expression in keratinocytes after DPM stimulation. Keratinocytes were cultured to approximately 90% confluence followed by pretreatment with 150 µM naringenin (Sigma-Aldrich) for 1 h before the addition DPM, 10 µg/mL (1650b, National Institute of Standards and Technology). The keratinocytes were then cultured in the presence of DPM and 150 µM naringenin for an additional 5 h. Assay is considered valid when the biomarker in question is significantly higher after stimulation than the untreated vehicle control. Cells are in parallel treated with the inhibitor quercetin, 10 µM, as a functional assay control.

#### 2.6. RNA Isolation and cDNA Synthesis

Total RNA was isolated using the RNeasy<sup>®</sup> Mini Kit (Qiagen, Hilden, Germany) and reverse transcription of RNA was performed with the iScript<sup>™</sup> Advanced cDNA Synthesis Kit (BioRad, Hercules, CA, USA) all according to the manufacturer's instructions.

#### 2.7. qPCR Analysis of CYP1A1 Gene Expression

The qPCR reaction was performed in a total volume of 20 µL containing 10 µL of SsoAdvanced<sup>™</sup> Universal SYBR<sup>®</sup> Green Supermix (BioRad), cDNA and the PrimePCR<sup>™</sup> SYBR<sup>®</sup> CYP1A1 (BioRad). The thermal cycling was carried out in a CFX96 ThermalCycler (BioRad) with a program of 95 °C for 3 min, followed by 40 cycles with denaturation at 95 °C for 10 s, and annealing and elongation at 55 °C for 30 s. The gene expression levels were normalized to the expression level of GAPDH housekeeping gene (PrimePCR<sup>™</sup> SYBR<sup>®</sup> GAPDH, BioRad). Relative gene expression changes, calculated using the  $2^{-\Delta\Delta CT}$  method, are reported as number-fold changes compared to those in the control samples.

#### 2.8. Gene Expression Analysis of Pigmentation Genes in Melanocytes

The melanocytes were cultured to approximately 90% confluence and thereafter cultured in the presence of naringenin (Sigma-Aldrich), 150 µM, or vehicle control (water) for 24 h. Total RNA was isolated from primary melanocytes using the RNeasy<sup>®</sup> Mini Kit (Qiagen). Nanostring hybridization was set up according to manufacturer's instructions, 25 ng RNA/reaction (nCounter<sup>®</sup> XT assay, nanoString Technologies, Seattle, WA, USA). Nanostring analysis was performed at KIGene core facility, CMM, Karolinska In-

stitutet, Sweden. Gene expression analysis of 27 selected melanogenesis genes (*MITF*, *ADRB2*, *CDH1*, *CTNNB1*, *DCT*, *DCTN1*, *EDN1*, *EDNRB*, *GPR143*, *GRIN1*, *GSTP1*, *HMOX1*, *KIT*, *MAPK1*, *MAPK3*, *MC1R*, *MLANA*, *MLPH*, *MYO5A*, *NFE2L2*, *PMEL*, *POMC*, *SFRP2*, *TYR*, *TYRP1*, *WNT3*, *WNT7A*) normalized to the two housekeeping genes, *GAPDH* and *PGK1*. Statistical analysis was performed by use of the software nSolver 3.0 (nanoString Technologies, USA)

## 2.9. Pigmentation Analysis, Reconstructed Human Epidermis

### 2.9.1. Cell Culture and Reconstruction of Epidermis

The study was conducted by Straticell, Gembloux, Belgium, using reconstructed human epidermis (RHE/MEL/001) that contained normal human keratinocytes and normal, darkly pigmented epidermal melanocytes. The RHE/MEL/001 was reconstructed at the air–liquid interface in EpiLife growth media supplemented with HKGS (Gibco) for 14 days in a humid atmosphere at 37 °C and 5% CO<sub>2</sub>. Bovine pituitary extract (BPE, Gibco) was added to the media at a concentration of 50 µg/mL from day 0 to day 4, and from day 5 to day 14, the media was supplemented without BPE.

### 2.9.2. Pigmentation Assay, with or without UV Challenge

Naringenin (Sigma-Aldrich) was applied topically in butylene glycol to the reconstructed skin at 0.5% and 0.1%. Application was done at six occasions during 10 days on day 4, 7, 8, 9, 10 and 11. In the UV challenge model the RHE/MEL/001 was treated with  $\alpha$ -MSH, 1 µM; on day 7, 8, 9, 10 and 11 in combination with UVA, 1 J/cm<sup>2</sup>; and UVB, 50 mJ/cm<sup>2</sup>, on day 8, 9, 10 and 11. Analysis took place on day 14. In parallel, the effect of kojic acid, 250 µM, (added systemically to the RHE/MEL/001) was measured as a reference compound to validate the analysis. At the end of treatments, melanin was extracted using Solvable (Perkin Elmer, Waltham, MA, USA), heated at 80 °C for 1 h and quantified spectrophotometrically at 490 nm. Synthetic melanin (Sigma-Aldrich) was used for standard curve. All data were compared to untreated control or vehicle control (butylene glycol) with or without UV challenge.

## 2.10. Statistical Analysis

Quantitative data are represented as mean  $\pm$  SEM. To analyze the statistical difference between two groups, two-sided Student's *t*-tests were used for the comparisons. For two or more groups, one-way analysis of variance (ANOVA) with Tukey's multiple-comparison test was used to analyze the statistical difference. Two-way ANOVA was chosen for analyzing the statistical difference between data points in groups. GraphPad Prism (GraphPad Software Inc., San Diego, CA, USA) was used for data analysis and graphic presentations.  $p^* \leq 0.05$ ,  $p^{**} \leq 0.01$  and  $p^{***} \leq 0.001$ .

## 3. Results

### 3.1. Viability

No decrease in cell viability was observed in either keratinocytes or fibroblasts after 24 h of treatment with naringenin up to a concentration of 150 µM. Therefore, this concentration was selected for use throughout the entire study.

### 3.2. Naringenin Inhibits UVB Induced Inflammatory Response in Human Primary Skin Cells

Abnormal induction of MMP-1 plays an important role in UV-induced photoaging through its degradation of collagen in dermal skin [4,23]. UVB induced MMP1 production was significantly inhibited after 1 h pretreatment, followed by 24 h treatment with naringenin in human primary dermal fibroblasts, as shown in Figure 2a. This inhibition is dose-dependent, with an IC<sub>50</sub> (50% inhibition concentration) of 1.4 µM of naringenin, as shown in Figure 2b.

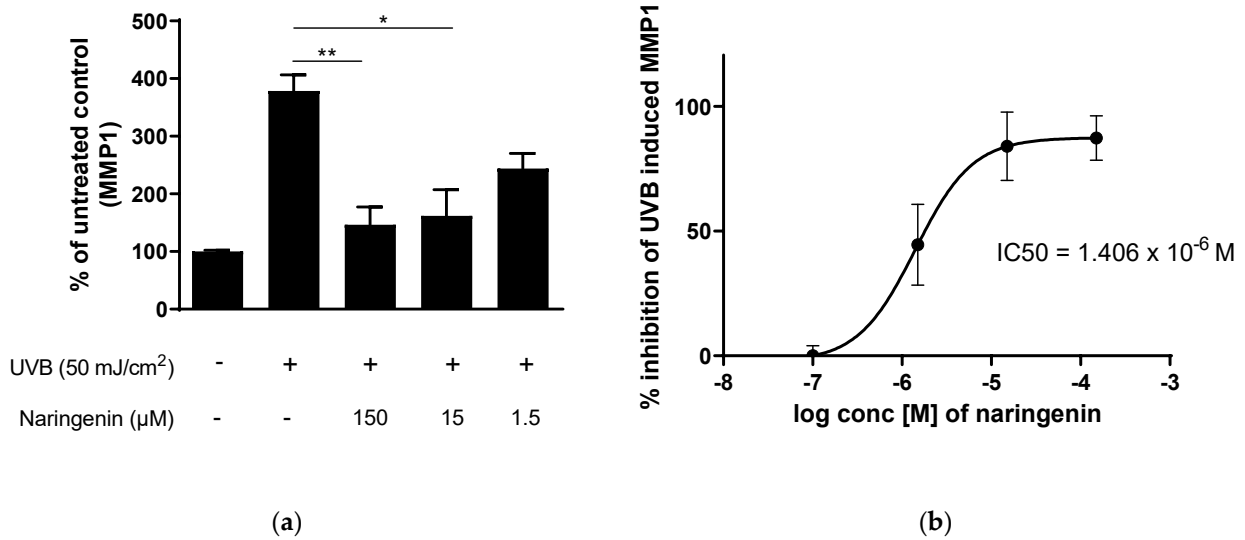


**Figure 2.** (a) Human dermal fibroblasts pre-treated for 1 h with naringenin 150 μM, 15 μM or 1.5 μM and then treated for 24 h with naringenin and media from UVB irradiated keratinocytes (50 mJ/cm<sup>2</sup>). MMP1 concentration presented as % of untreated control. Statistics were performed on raw data with unpaired student’s *t*-test, where  $p^* \leq 0.05$ , and  $p^{**} \leq 0.01$ .  $n = 3$ , where  $n$  is the number of fibroblast donors. (b) Concentration of naringenin (log) was plotted against % inhibition of UVB-induced MMP1. The IC<sub>50</sub> for naringenin’s ability to inhibit UVB induced MMP1 in dermal human fibroblasts was calculated to be 1.4 μM.

In addition to inhibition of MMP1, naringenin also significantly inhibited UVB-induced MMP3, IL-6 and GM-CSF, as shown in Figure 3. They have all been shown to be upregulated in skin after UV irradiation and involved in the inflammation and photoaging process of the skin [24–26].

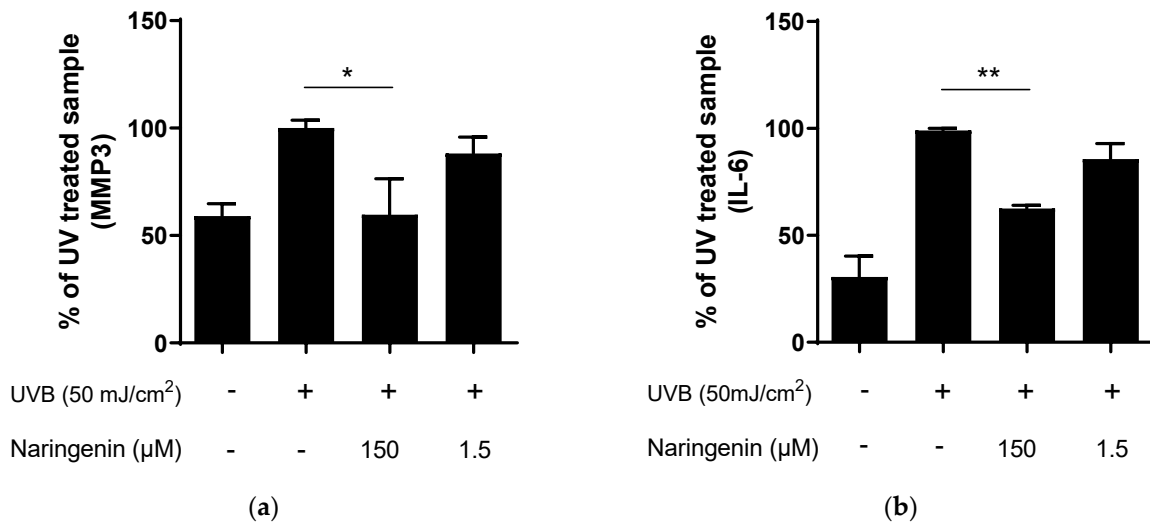


**Figure 3.** Cont.

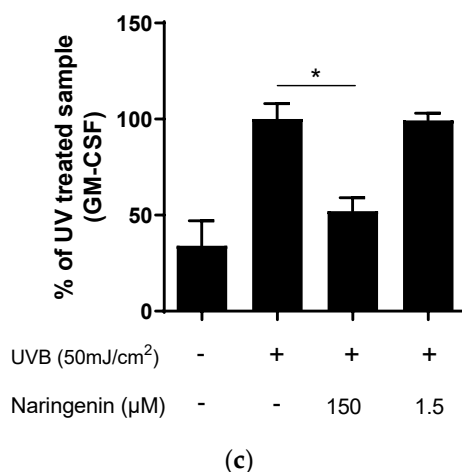


**Figure 3.** Human dermal fibroblasts pre-treated for 1 h with naringenin 150 µM or 1.5 µM and then treated for 24 h with naringenin in media from UVB irradiated keratinocytes (50 mJ/cm<sup>2</sup>). (a) MMP3 concentration presented as % of UV-treated sample. (b) IL-6 concentration presented as % of UV-treated sample. (c) GM-CSF concentration presented as % of UV-treated sample. Statistics were performed on raw data with unpaired student's *t*-test, where  $p^* \leq 0.05$  and  $p^{**} \leq 0.01$ .  $n = 2$  in duplicates where  $n$  is the number of fibroblast donors.

### 3.3. Naringenin Inhibits Pollution-Induced MMP1 in Human Dermal Fibroblasts

As shown in previous studies, pollution induced activation of the AhR pathway activate MMP-1 expression in human fibroblasts and keratinocytes [9], thus contributing to matrix degradation and extrinsic aging. Here, we show that naringenin significantly inhibits DPM-induced MMP1 expression in human primary fibroblasts, as shown in Figure 4.

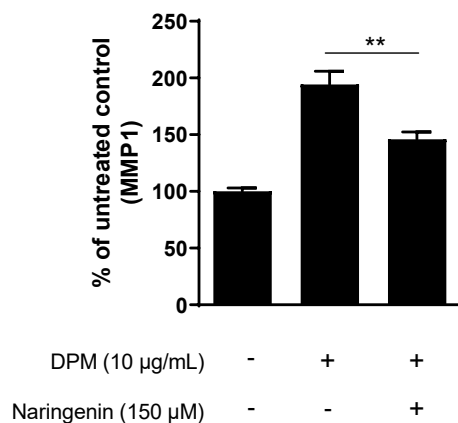


**Figure 4.** Human dermal fibroblasts pre-treated for 1 h with 150 µM naringenin, and then treated for 24 h with naringenin and media from DPM treated (10 µg/mL) keratinocytes. MMP1 concentration presented as % of untreated control. Statistics were performed on raw data with unpaired student's *t*-test, where  $p^{**} \leq 0.01$ .  $n = 3$ , where  $n$  is the number of fibroblast donors.

### 3.4. Naringenin Inhibits Pollution-Induced CYP1A1 in Human Keratinocytes

Air pollution has been shown to increase the expression of the *CYP1A1* gene, which belongs to the P450 family of enzymes. When activated, *CYP1A1* metabolizes environmental pollutants into highly reactive intermediates that can cause DNA damage, oxidative stress, and inflammation [27,28]. In this study, we demonstrate that *CYP1A1* expression is upregulated after exposure to diesel particulate matter (DPM). Primary human keratinocytes were treated with DPM for 5 h, resulting in a significant 14-fold increase in *CYP1A1* expression compared to the control group; however, pre-treatment with 150 µM

naringenin for 1 h followed by 5 h of combined naringenin and DPM exposure resulted in a significant downregulation of *CYP1A1* gene expression back to basal levels (Figure 5).

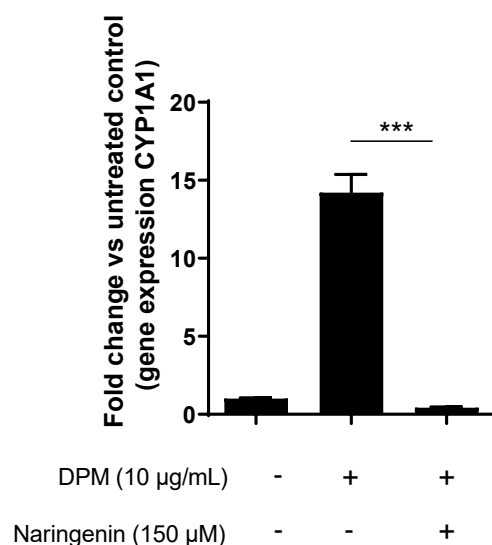


**Figure 5.** Human dermal keratinocytes pre-treated for 1 h with naringenin 150 µM, and then treated for 5 h with naringenin and DPM (10 µg/mL). Gene expression presented as fold change compared to untreated control. Statistics were performed on  $\Delta\text{Ct}$ .  $n = 3$ , where  $n$  is the number of keratinocyte donors. Unpaired student's  $t$ -test, where  $p^{***} \leq 0.001$ .

### 3.5. Naringenin Downregulates Key Melanogenesis Genes

To investigate the effect of naringenin on genes involved in melanogenesis, we treated melanocytes with naringenin for 24 h and analyzed the gene expression of 27 melanogenesis-associated genes.

Three of these genes, *MITE*, *MLPH* and *MYO5A*, were significantly downregulated by naringenin compared to the vehicle (Table 1).

**Table 1.** Gene expression analysis in primary human melanocytes treated with 150 µM naringenin for 24 h. Statistical analysis was performed by use of the software nSolver 3.0 (NanoString Technologies, USA),  $n = 1$  in duplicates, where  $n$  is the number of melanocyte donors.

Gene ID	Naringenin	Vehicle	Ratio	$p$ Value
MLPH XM_006712737.1	192.88	226.91	0.85	0.049
	159.27	226.91	0.7	0.028
MYO5A NM_000259.3	544.97	808.06	0.67	0.03
	549.92	808.06	0.68	0.024
MITF NM_000248.3	298.35	401.2	0.74	0.026
	302.99	401.2	0.76	0.049

### 3.6. Naringenin Inhibits Basal and UV-Induced Melanogenesis in Human Pigmented Reconstructed Epidermis

#### 3.6.1. Visual Analysis

The macroscopic pictures show that systemic treatment with the control compound kojic acid results in whitening of the tissue compared to untreated, both with and without UV. It can also be concluded that topical treatment with naringenin results in a visual whitening effect compared to vehicle both with and without UV, Figure 6.

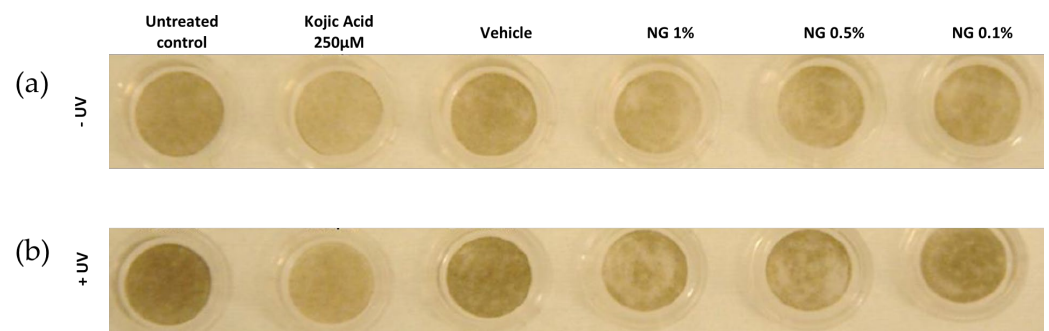


**Figure 6.** Macroscopic picture of RHE/MEL tissues treated systemically with kojic acid or topically with naringenin (NG) or vehicle (butylene glycol) for 10 days (from day 4 to 14), without (a) or with UVA (1 J/cm<sup>2</sup>), UVB (50 mJ/cm<sup>2</sup>) and  $\alpha$ -MSH (1  $\mu$ M) (b).

### 3.6.2. Melanin Content Analysis after Chemical Extraction

Following the visual analysis, melanin was extracted from the RHE/MEL tissues at the end of treatments on day 14 and quantified spectrophotometrically. The level of melanin in the untreated samples without UV was as expected lower than in the UVA/UVB +  $\alpha$ -MSH-treated tissues, 33  $\mu$ g/mL compared to 53  $\mu$ g/mL (Figure 7a and 7b, respectively). Treatment with the control compound kojic acid significantly decreased the melanin content in epidermis both with and without UV challenge, validating the experimental setup.

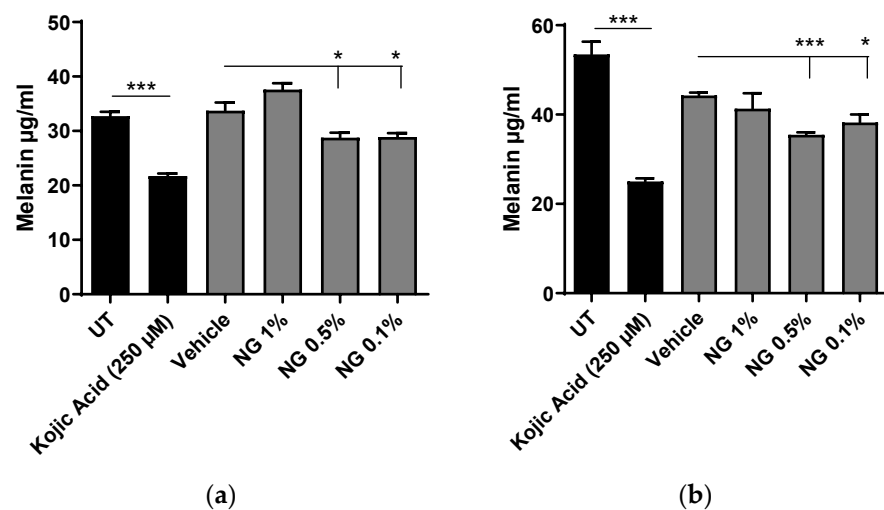


**Figure 7.** Quantification of extracted melanin from reconstructed human epidermis containing melanocytes. Topically treated for 10 days with naringenin (NG) or systemically with the control compound kojic acid (KA), without (a) or with UVA/B (b). The histograms represent values obtained from three tissues ( $n = 3$ ) for each treatment. For statistical analysis, a student's  $t$ -test was performed, where  $p^* \leq 0.05$ , and  $p^{***} \leq 0.001$ .

Topical treatment with naringenin, 0.5% and 0.1%, also results in a significant decrease in melanin both with and without UV. At 1%, visual effects are observed from the macroscopic pictures but could not be confirmed after melanin extraction (Figure 6a,b).

## 4. Discussion

Naringenin, a flavonoid that is commonly found in citrus fruits, has been demonstrated to possess various beneficial properties for the skin. These include antioxidant, anti-inflammatory, and anticancer effects, as reported in previous studies [29–31]. Furthermore, topical application of naringenin has been shown to reduce skin inflammation and oxidative stress caused by UVB radiation in mice [19].

The primary aim of this study was to thoroughly investigate the protective and restorative effects of naringenin on human primary skin cells and reconstructed skin when exposed to external stressors, thus shedding light on its potential in promoting overall skin health. Throughout this study, we specifically utilized primary skin cells due to their inherent advantages, such as better functionality and the ability to exhibit more accurate physiological responses, as compared to cell lines commonly used in research. Additionally, the utilization of reconstructed skin models in this study further enhanced the relevance and translatability of our findings.

UV radiation is a known cause of skin damage, resulting in premature aging, wrinkles, and an increased risk of skin cancer. In the context of skin aging and photoaging, an increase in matrix metalloproteinases plays a critical role in the unbalanced turnover or rapid breakdown of collagen and elastin fibers in the skin, leading to the development of fine lines, wrinkles, and loss of elasticity [4].

In this study, we investigated the effect of naringenin on two of these matrix metalloproteinases (MMPs), MMP1 and MMP3, which are known to be upregulated in response to UV radiation in human skin cells. MMP1 is considered the major collagenase involved in photoaging caused by UV irradiation [23,24]. In line with previous results showing MMP1 inhibition in rat, mice, and human cell lines, [32–35], we showed a significant inhibition of UVB induced MMP1 production in human primary fibroblasts, as shown in Figure 2a. Moreover, this downregulation was found to be dose-dependent, and an IC50 value of 1.4  $\mu$ M was established for MMP1, as shown in Figure 2b.

In addition to MMP1 inhibition, we also demonstrate that naringenin significantly reduces the UVB-induced increase in MMP3, Figure 3a, in human primary fibroblasts. MMP3, also plays a crucial role in tissue remodeling and degradation of the extracellular matrix [36]. MMP3 has also been linked to inflammatory processes in the skin and excessive MMP3 activity can promote the release of pro-inflammatory cytokines and chemokines, triggering an inflammatory response [37].

Interleukin-6 (IL-6) and granulocyte-macrophage colony-stimulating factor (GM-CSF) are both cytokines involved in immune responses and inflammation. While these cytokines play important roles in the immune system, excessive or dysregulated levels of IL-6 and GM-CSF can have negative effects on the skin. They are both pro-inflammatory cytokines that can contribute to chronic inflammation when their levels are elevated and prolonged inflammation in the skin can lead to tissue damage, impaired skin barrier function, and the development of various skin disorders. Elevated levels of IL-6 and GM-CSF have also been associated with skin aging, by promoting the production of MMPs and elastase, leading to reduced skin elasticity, increased wrinkles, and loss of skin firmness [38,39].

Both IL-6 and GM-CSF are known to be upregulated by UVB radiation in the skin [25,26]. In this study we demonstrate that following treatment with naringenin, the UVB-induced levels of IL-6 and GM-CSF were normalized (Figure 3b and 3c, respectively). Collectively, these findings in human primary skin fibroblasts support previous studies conducted in animal models and in a human cell line that have shown the photoprotective properties of naringenin [19,30,32,40].

Like UV radiation, air pollution also leads to an increase of intracellular reactive oxygen species (ROS), inflammatory mediators, pro-inflammatory cytokines, and matrix metalloproteinases in the skin. Moreover, pollution can interact with UV radiation and have synergistic effects on the skin, leading to more pronounced damage [41]. The effect of pollution to the skin is primarily due to the direct activation of the aryl hydrocarbon receptor (AhR) [7–10]. One of the downstream genes that is directly activated by pollution via the AhR is *CYP1A1*, which belongs to the cytochrome P450 family of enzymes that play a role in the metabolism of various xenobiotics, including polycyclic aromatic hydrocarbons (PAHs) that are present in cigarette smoke and air pollution. The activation of *CYP1A1* increases the metabolism of these compounds, resulting in their detoxification and elimination from the body. However, *CYP1A1* also catalyzes the conversion of the common exhaust pollutant benzo[a]pyrene (B[a]P) into the highly toxic epoxide (BP-7,8-

dihydrodiol-9,10-epoxide). Thus, inhibiting *CYP1A1* may be of interest to protect the skin from pollution-induced damage [8,42]. In this study, we demonstrated that naringenin inhibits both pollution-induced upregulation of MMP1 in human fibroblasts (Figure 4) and AhR-mediated upregulation of *CYP1A1* expression (Figure 5).

In addition to causing oxidative stress, inflammation, and premature skin aging, UV and polluted air can lead to uneven skin tone and hyperpigmentation [5,43,44]. Previous studies reported that naringenin can both stimulate and inhibit melanogenesis [45–48]; however, they were conducted in murine melanoma cells. In our study, we demonstrate that in human primary melanocytes, naringenin acts as an inhibitor of several key melanogenesis genes (Table 1). Microphthalmia-associated transcription factor (MITF) is a master regulator of melanocyte development, differentiation, and function. It regulates the expression of several genes involved in melanogenesis, including TYR, TYRP1, DCT, and PMEL, which are necessary for melanin production [49]. Overexpression or hyperactivation of MITF can lead to hyperpigmentation. Melanophilin (MLPH) and myosin 5 (MYO5A) both play essential roles in melanogenesis by regulating the maturation and transport of melanosomes and maintaining the proper distribution of melanin in the skin [50,51]. Furthermore, we show that when topically applied to reconstructed pigmented epidermis with human primary cells, naringenin significantly reduces pigmentation (Figures 6 and 7).

## 5. Conclusions

In conclusion, this study confirms naringenin's photoprotective properties in human primary skin cells and, to our knowledge, for the first time, demonstrates its ability to protect against pollution-induced skin damage by inhibiting MMP1 as well as *CYP1A1*. In combination with naringenin's ability to reduce pigmentation, it counteracts some of the major hallmarks of extrinsic aging caused by UVB and pollution. Overall, given the protective effects of naringenin against both UVB radiation and pollution-induced skin damage, it holds great promise as a candidate for the development of skincare products.

**Author Contributions:** Conceptualization and supervision, L.V.-J.; methodology, N.H., V.L.-K., N.A., S.S. and C.Ö.; formal analysis, C.Ö.; investigation, C.Ö., N.H., V.L.-K. and N.A.; data curation, C.Ö.; writing—original draft preparation, C.Ö.; writing—review and editing, C.Ö., N.H., N.A., S.S. and L.V.-J. All authors have read and agreed to the published version of the manuscript.

**Funding:** This research received no external funding.

**Institutional Review Board Statement:** Not applicable.

**Informed Consent Statement:** Not applicable.

**Data Availability Statement:** The data presented in this study are available upon request from the corresponding author.

**Conflicts of Interest:** The authors declare no conflict of interest.

## References

1. Krutmann, J.; Liu, W.; Li, L.; Pan, X.; Crawford, M.; Sore, G.; Seite, S. Pollution and Skin: From Epidemiological and Mechanistic Studies to Clinical Implications. *J. Dermatol. Sci.* **2014**, *76*, 163–168. [[CrossRef](#)] [[PubMed](#)]
2. Velasco, M.V.R.; Sauce, R.; de Oliveira, C.A.; de Oliveira Pinto, C.A.S.; Martinez, R.M.; Baah, S.; Almeida, T.S.; Rosado, C.; Baby, A.R. Active Ingredients, Mechanisms of Action and Efficacy Tests of Antipollution Cosmetic and Personal Care Products. *Brazilian J. Pharm. Sci.* **2018**, *54*, e01003. [[CrossRef](#)]
3. Khmaladze, I.; Leonardi, M.; Fabre, S.; Messaraa, C.; Mavon, A. The Skin Interactome: A Holistic “Genome-Microbiome-Exposome” Approach to Understand and Modulate Skin Health and Aging. *Clin. Cosmet. Investig. Dermatol.* **2020**, *13*, 1021–1040. [[CrossRef](#)] [[PubMed](#)]
4. Fisher, G.J.; Kang, S.; Varani, J.; Bata-Csorgo, Z.; Wan, Y.; Datta, S.; Voorhees, J.J. Mechanisms of Photoaging and Chronological Skin Aging. *Arch. Dermatol.* **2002**, *138*, 1462–1470. [[CrossRef](#)] [[PubMed](#)]
5. Vierkötter, A.; Schikowski, T.; Ranft, U.; Sugiri, D.; Matsui, M.; Krämer, U.; Krutmann, J. Airborne Particle Exposure and Extrinsic Skin Aging. *J. Investig. Dermatol.* **2010**, *130*, 2719–2726. [[CrossRef](#)]

6. Ahn, Y.; Lee, E.J.; Luo, E.; Choi, J.; Kim, J.Y.; Kim, S.; Kim, S.H.; Bae, Y.J.; Park, S.; Lee, J.; et al. Particulate Matter Promotes Melanin Production through Endoplasmic Reticulum Stress-Mediated IRE1 $\alpha$  Signaling. *J. Investig. Dermatol.* **2022**, *142*, 1425–1434. [\[CrossRef\]](#)
7. Nguyen, L.P.; Bradfield, C.A. The Search for Endogenous Activators of the Aryl Hydrocarbon Receptor. *Chem. Res. Toxicol.* **2008**, *21*, 102–116. [\[CrossRef\]](#)
8. Costa, C.; Catania, S.; De Pasquale, R.; Stancanelli, R.; Scribano, G.M.; Melchini, A. Exposure of Human Skin to Benzo[a]Pyrene: Role of CYP1A1 and Aryl Hydrocarbon Receptor in Oxidative Stress Generation. *Toxicology* **2010**, *271*, 83–86. [\[CrossRef\]](#)
9. Ono, Y.; Torii, K.; Fritsche, E.; Shintani, Y.; Nishida, E.; Nakamura, M.; Shirakata, Y.; Haarmann-Stemann, T.; Abel, J.; Krutmann, J.; et al. Role of the Aryl Hydrocarbon Receptor in Tobacco Smoke Extract-Induced Matrix Metalloproteinase-1 Expression. *Exp. Dermatol.* **2013**, *22*, 349–353. [\[CrossRef\]](#)
10. Tigges, J.; Haarmann-Stemann, T.; Vogel, C.F.A.; Grindel, A.; Hübenthal, U.; Brenden, H.; Grether-Beck, S.; Vielhaber, G.; Johncock, W.; Krutmann, J.; et al. The New Aryl Hydrocarbon Receptor Antagonist E/Z-2-Benzylindene-5,6-Dimethoxy-3,3-Dimethylindan-1-One Protects against UVB-Induced Signal Transduction. *J. Investig. Dermatol.* **2014**, *134*, 556–559. [\[CrossRef\]](#)
11. Barreca, D.; Mandalari, G.; Calderaro, A.; Smeriglio, A.; Trombetta, D.; Felice, M.R.; Gattuso, G. Citrus Flavones: An Update on Sources, Biological Functions, and Health Promoting Properties. *Plants* **2020**, *9*, 288. [\[CrossRef\]](#)
12. de Lima Cherubim, D.J.; Buzanello Martins, C.V.; Oliveira Fariña, L.; da Silva de Lucca, R.A. Polyphenols as Natural Antioxidants in Cosmetics Applications. *J. Cosmet. Dermatol.* **2020**, *19*, 33–37. [\[CrossRef\]](#)
13. Panche, A.N.; Diwan, A.D.; Chandra, S.R. Flavonoids: An Overview. *J. Nutr. Sci.* **2016**, *5*, e47. [\[CrossRef\]](#)
14. Nunes, A.R.; Vieira, Í.G.P.; Queiroz, D.B.; Leal, A.L.A.B.; Maia Morais, S.; Muniz, D.F.; Calixto-Junior, J.T.; Coutinho, H.D.M. Use of Flavonoids and Cinnamates, the Main Photoprotectors with Natural Origin. *Adv. Pharmacol. Sci.* **2018**, *2018*, 5341487. [\[CrossRef\]](#)
15. Takayama, K.S.; Monteiro, M.C.; Saito, P.; Pinto, I.C.; Nakano, C.T.; Martinez, R.M.; Thomaz, D.V.; Verri, W.A.; Baracat, M.M.; Arakawa, N.S.; et al. Rosmarinus Officinalis Extract-Loaded Emulgel Prevents UVB Irradiation Damage to the Skin. *An. Acad. Bras. Cienc.* **2022**, *94*, e20201058. [\[CrossRef\]](#)
16. Velasco, M.V.R.; Sarruf, F.D.; Salgado-Santos, I.M.N.; Haroutiounian-Filho, C.A.; Kaneko, T.M.; Baby, A.R. Broad Spectrum Bioactive Sunscreens. *Int. J. Pharm.* **2008**, *363*, 50–57. [\[CrossRef\]](#)
17. Lee, C.-H.; Jeong, T.-S.; Choi, Y.-K.; Hyun, B.-H.; Oh, G.-T.; Kim, E.-H.; Kim, J.-R.; Han, J.-I.; Bok, S.-H. Anti-Atherogenic Effect of Citrus Flavonoids, Naringin and Naringenin, Associated with Hepatic ACAT and Aortic VCAM-1 and MCP-1 in High Cholesterol-Fed Rabbits. *Biochem. Biophys. Res. Commun.* **2001**, *284*, 681–688. [\[CrossRef\]](#)
18. Al-Roujayee, A.S. Naringenin Improves the Healing Process of Thermally-Induced Skin Damage in Rats. *J. Int. Med. Res.* **2017**, *45*, 570–582. [\[CrossRef\]](#)
19. Martinez, R.M.; Pinho-Ribeiro, F.A.; Steffen, V.S.; Silva, T.C.C.; Caviglione, C.V.; Bottura, C.; Fonseca, M.J.V.; Vicentini, F.T.M.C.; Vignoli, J.A.; Baracat, M.M.; et al. Topical Formulation Containing Naringenin: Efficacy against Ultraviolet B Irradiation-Induced Skin Inflammation and Oxidative Stress in Mice. *PLoS ONE* **2016**, *11*, e0146296. [\[CrossRef\]](#)
20. Pinho-Ribeiro, F.A.; Zarpelon, A.C.; Fattori, V.; Manchope, M.F.; Mizokami, S.S.; Casagrande, R.; Verri, W.A. Naringenin Reduces Inflammatory Pain in Mice. *Neuropharmacology* **2016**, *105*, 508–519. [\[CrossRef\]](#)
21. Ali, R.; Shahid, A.; Ali, N.; Hasan, S.K.; Majed, F.; Sultana, S. Amelioration of Benzo[a]Pyrene-Induced Oxidative Stress and Pulmonary Toxicity by Naringenin in Wistar Rats: A Plausible Role of COX-2 and NF-KB. *Hum. Exp. Toxicol.* **2016**, *36*, 349–364. [\[CrossRef\]](#) [\[PubMed\]](#)
22. Wang, X.; Bi, Z.; Chu, W.; Wan, Y. IL-1 Receptor Antagonist Attenuates MAP Kinase/AP-1 Activation and MMP1 Expression in UVA-Irradiated Human Fibroblasts Induced by Culture Medium from UVB-Irradiated Human Skin Keratinocytes. *Int. J. Mol. Med.* **2005**, *16*, 1117–1124. [\[CrossRef\]](#) [\[PubMed\]](#)
23. Brennan, M.; Bhatti, H.; Nerusu, K.C.; Bhagavathula, N.; Kang, S.; Fisher, G.J.; Varani, J.; Voorhees, J.J. Matrix Metalloproteinase-1 Is the Major Collagenolytic Enzyme Responsible for Collagen Damage in UV-Irradiated Human Skin. *Photochem. Photobiol.* **2007**, *78*, 43–48. [\[CrossRef\]](#)
24. Lu, J.; Guo, J.H.; Tu, X.L.; Zhang, C.; Zhao, M.; Zhang, Q.W.; Gao, F.H. Tiron Inhibits UVB-Induced AP-1 Binding Sites Transcriptional Activation on MMP-1 and MMP-3 Promoters by MAPK Signaling Pathway in Human Dermal Fibroblasts. *PLoS ONE* **2016**, *11*, e0159998. [\[CrossRef\]](#)
25. Choi, Y.J.; Uehara, Y.; Park, J.Y.; Kim, S.J.; Kim, S.R.; Lee, H.W.; Moon, H.R.; Chung, H.Y. MHY884, a Newly Synthesized Tyrosinase Inhibitor, Suppresses UVB-Induced Activation of NF-KB Signaling Pathway through the Downregulation of Oxidative Stress. *Bioorg. Med. Chem. Lett.* **2014**, *24*, 1344–1348. [\[CrossRef\]](#)
26. Sharma, S.D.; Katiyar, S.K. Dietary Grape Seed Proanthocyanidins Inhibit UVB-Induced Cyclooxygenase-2 Expression and Other Inflammatory Mediators in UVB-Exposed Skin and Skin Tumors of SKH-1 Hairless Mice. *Pharm. Res.* **2010**, *27*, 1092–1102. [\[CrossRef\]](#)
27. Nebert, D.W.; Dalton, T.P.; Okey, A.B.; Gonzalez, F.J. Role of Aryl Hydrocarbon Receptor-Mediated Induction of the CYP1 Enzymes in Environmental Toxicity and Cancer. *J. Biol. Chem.* **2004**, *279*, 23847–23850. [\[CrossRef\]](#)
28. Furue, M.; Uchi, H.; Mitoma, C.; Hashimoto-Hachiya, A.; Tanaka, Y.; Ito, T.; Tsuji, G. Implications of Tryptophan Photoproduct FICZ in Oxidative Stress and Terminal Differentiation of Keratinocytes. *G. Ital. Dermatol. Venereol.* **2019**, *154*, 37–41. [\[CrossRef\]](#)

29. Manchope, M.F.; Casagrande, R.; Verri, W.A. Naringenin: An Analgesic and Anti-Inflammatory Citrus Flavanone. *Oncotarget* **2017**, *8*, 3766–3767. [[CrossRef](#)]
30. Kumar, R.; Bhan Tikku, A. Naringenin Suppresses Chemically Induced Skin Cancer in Two-Stage Skin Carcinogenesis Mouse Model. *Nutr. Cancer* **2020**, *72*, 976–983. [[CrossRef](#)]
31. Sun, R.; Liu, C.; Liu, J.; Yin, S.; Song, R.; Ma, J.; Cao, G.; Lu, Y.; Zhang, G.; Wu, Z.; et al. Integrated Network Pharmacology and Experimental Validation to Explore the Mechanisms Underlying Naringenin Treatment of Chronic Wounds. *Sci. Rep.* **2023**, *13*, 132. [[CrossRef](#)]
32. Jung, S.K.; Ha, S.J.; Jung, C.H.; Kim, Y.T.; Lee, H.K.; Kim, M.O.; Lee, M.H.; Mottamal, M.; Bode, A.M.; Lee, K.W.; et al. Naringenin Targets ERK2 and Suppresses UVB-Induced Photoaging. *J. Cell. Mol. Med.* **2016**, *20*, 909–919. [[CrossRef](#)]
33. Martinez, R.M.; Pinho-Ribeiro, F.A.; Steffen, V.S.; Caviglione, C.V.; Vignoli, J.A.; Barbosa, D.S.; Baracat, M.M.; Georgetti, S.R.; Verri, W.A.; Casagrande, R. Naringenin Inhibits UVB Irradiation-Induced Inflammation and Oxidative Stress in the Skin of Hairless Mice. *J. Nat. Prod.* **2015**, *78*, 1647–1655. [[CrossRef](#)]
34. Chang, H.L.; Chang, Y.M.; Lai, S.C.; Chen, K.M.; Wang, K.C.; Chiu, T.T.; Chang, F.H.; Hsu, L.S. Naringenin Inhibits Migration of Lung Cancer Cells via the Inhibition of Matrix Metalloproteinases-2 and-9. *Exp. Ther. Med.* **2017**, *13*, 739–744. [[CrossRef](#)]
35. Wang, C.C.; Guo, L.; Tian, F.D.; An, N.; Luo, L.; Hao, R.H.; Wang, B.; Zhou, Z.H. Naringenin Regulates Production of Matrix Metalloproteinases in the Knee-Joint and Primary Cultured Articular Chondrocytes and Alleviates Pain in Rat Osteoarthritis Model. *Brazilian. J. Med. Biol. Res.* **2017**, *50*, e5714. [[CrossRef](#)]
36. Quan, T.; Little, E.; Quan, H.; Qin, Z.; Voorhees, J.J.; Fisher, G.J. Elevated Matrix Metalloproteinases and Collagen Fragmentation in Photodamaged Human Skin: Impact of Altered Extracellular Matrix Microenvironment on Dermal Fibroblast Function. *J. Investig. Dermatol.* **2013**, *133*, 1362. [[CrossRef](#)]
37. Fingleton, B. Matrix Metalloproteinases as Regulators of Inflammatory Processes. *Biochim. Biophys. Acta Mol. Cell. Res.* **2017**, *1864*, 2036–2042. [[CrossRef](#)]
38. Onodera, S.; Kaneda, K.; Mizue, Y.; Koyama, Y.; Fujinaga, M.; Nishihira, J. Macrophage Migration Inhibitory Factor Up-Regulates Expression of Matrix Metalloproteinases in Synovial Fibroblasts of Rheumatoid Arthritis. *J. Biol. Chem.* **2000**, *275*, 444–450. [[CrossRef](#)]
39. Imokawa, G.; Nakajima, H.; Ishida, K. Biological Mechanisms Underlying the Ultraviolet Radiation-Induced Formation of Skin Wrinkling and Sagging II: Over-Expression of Neprilysin Plays an Essential Role. *Int. J. Mol. Sci.* **2015**, *16*, 7776–7795. [[CrossRef](#)]
40. El-Mahdy, M.A.; Zhu, Q.; Wang, Q.E.; Wani, G.; Patnaik, S.; Zhao, Q.; Arafa, E.S.; Barakat, B.; Mir, S.N.; Wani, A.A. Naringenin Protects HaCaT Human Keratinocytes against UVB-Induced Apoptosis and Enhances the Removal of Cyclobutane Pyrimidine Dimers from the Genome. *Photochem. Photobiol.* **2008**, *84*, 307–316. [[CrossRef](#)]
41. Kim, K.E.; Cho, D.; Park, H.J. Air Pollution and Skin Diseases: Adverse Effects of Airborne Particulate Matter on Various Skin Diseases. *Life Sci.* **2016**, *152*, 126–134. [[CrossRef](#)] [[PubMed](#)]
42. Shimizu, Y.; Nakatsuru, Y.; Ichinose, M.; Takahashi, Y.; Kume, H.; Mimura, J.; Fujii-Kuriyama, Y.; Ishikawa, T. Benzo[a]Pyrene Carcinogenicity Is Lost in Mice Lacking the Aryl Hydrocarbon Receptor. *Proc. Natl. Acad. Sci. USA* **2000**, *97*, 779. [[CrossRef](#)] [[PubMed](#)]
43. Grether-Beck, S.; Felsner, I.; Brenden, H.; Marini, A.; Jaenicke, T.; Aue, N.; Welss, T.; Uthe, I.; Krutmann, J. Air Pollution-Induced Tanning of Human Skin. *Br. J. Dermatol.* **2021**, *185*, 1026–1034. [[CrossRef](#)] [[PubMed](#)]
44. Shi, Y.; Zeng, Z.; Liu, J.; Pi, Z.; Zou, P.; Deng, Q.; Ma, X.; Qiao, F.; Xiong, W.; Zhou, C.; et al. Particulate Matter Promotes Hyperpigmentation via AhR/MAPK Signaling Activation and by Increasing  $\alpha$ -MSH Paracrine Levels in Keratinocytes. *Environ. Pollut.* **2021**, *278*, 116850. [[CrossRef](#)] [[PubMed](#)]
45. Kim, S.S.; Kim, M.J.; Choi, Y.H.; Kim, B.K.; Kim, K.S.; Park, K.J.; Park, S.M.; Lee, N.H.; Hyun, C.G. Down-Regulation of Tyrosinase, TRP-1, TRP-2 and MITF Expressions by Citrus Press-Cakes in Murine B16 F10 Melanoma. *Asian Pac. J. Trop. Biomed.* **2013**, *3*, 617–622. [[CrossRef](#)]
46. Murata, K.; Takahashi, K.; Nakamura, H.; Itoh, K.; Matsuda, H. Search for Skin-Whitening Agent from Prunus Plants and the Molecular Targets in Melanogenesis Pathway of Active Compounds. *Nat. Prod. Commun.* **2014**, *9*, 185–188. [[CrossRef](#)]
47. Huang, Y.C.; Yang, C.H.; Chiou, Y.L. Citrus Flavanone Naringenin Enhances Melanogenesis through the Activation of Wnt/ $\beta$ -Catenin Signalling in Mouse Melanoma Cells. *Phytomedicine* **2011**, *18*, 1244–1249. [[CrossRef](#)]
48. Nasr Bouzaiane, N.; Chaabane, F.; Sassi, A.; Chekir-Ghedira, L.; Ghedira, K. Effect of Apigenin-7-Glucoside, Genkwanin and Naringenin on Tyrosinase Activity and Melanin Synthesis in B16F10 Melanoma Cells. *Life Sci.* **2016**, *144*, 80–85. [[CrossRef](#)]
49. Vance, K.W.; Goding, C.R. The Transcription Network Regulating Melanocyte Development and Melanoma. *Pigment. Cell. Res.* **2004**, *17*, 318–325. [[CrossRef](#)]
50. Wu, X.; Bowers, B.; Rao, K.; Wei, Q.; Hammer, J.A. Visualization of Melanosome Dynamics within Wild-Type and Dilute Melanocytes Suggests a Paradigm for Myosin V Function In Vivo. *J. Cell Biol.* **1998**, *143*, 1899–1918. [[CrossRef](#)]
51. Hume, A.N.; Ushakov, D.S.; Tarafder, A.K.; Ferenczi, M.A.; Seabra, M.C. Rab27a and MyoVa Are the Primary Mlph Interactors Regulating Melanosome Transport in Melanocytes. *J. Cell Sci.* **2007**, *120*, 3111–3122. [[CrossRef](#)]

**Disclaimer/Publisher’s Note:** The statements, opinions and data contained in all publications are solely those of the individual author(s) and contributor(s) and not of MDPI and/or the editor(s). MDPI and/or the editor(s) disclaim responsibility for any injury to people or property resulting from any ideas, methods, instructions or products referred to in the content.